# Generation and evaluation of projected moving patterns for reference-free BOS with increased spatial resolution

M. Raffel[1], N.T. Smith[2], C.C. Wolf[1], J.T. Heineck[3], A.D. Gardner[1]

1: Institute of Aerodynamics and Flow Technology, DLR Göttingen, Germany
2: Metis Technology Solutions Inc., Experimental Aero-Physics Branch, NASA Ames Research Center, Moffett Field, CA, USA
3: Experimental Aero-Physics Branch, NASA Ames Research Center, Moffett Field, CA, USA
* Correspondent author: Markus.Raffel@dlr.de

**Keywords:** BOS recording, BOS processing, schlieren technique, laser speckles, density gradients

ABSTRACT

A method of taking background oriented schlieren technique (BOS) images using projected backgrounds is shown. The projected backgrounds can be scaled to the measurement requirements, providing more flexibility than printed backgrounds. The evaluation of the BOS image pairs using cross correlation or optical flow analysis was shown to produce equivalent results. The background can be dynamically moved using a rotating mirror, allowing evaluation using the reference-free shadowgraphy or reference-free BOS methods. *Forward BOS* is shown, where the projected speckle pattern shines through the density object onto a screen, and is recorded by a camera focused on the screen. In contrast to standard shadowgraphy, this technique is robust when the lighting of the field is uneven, and the point movement is related to the first derivative of density.

## 1. Introduction

Background oriented schlieren (BOS) is a common density gradient imaging technique, with a large number of variants, summarized in Raffel (2015). A camera is focused on a printed background with a low self-correlating pattern ("random dot pattern"), which is visualized once without flow and once with flow. Moving-window cross-correlation and optical flow algorithms, identical to those used for particle image velocimetry (PIV) were used to analyze the images, and the movement of the background is related to the refractive index by:

$$\Delta y = f\left(\frac{Z_D}{Z_D+Z_A-f}\right)\frac{1}{n_0}\int_0^1 \frac{\partial n}{\partial y}\,dz \qquad (1)$$

and an equivalent equation gives the movement in the x axis. The background movement $\Delta y$ is a function of the z dimensions as detailed in Fig. 1, the camera focal length f and the index of refraction of the undisturbed background $n_0$ and of the object n, which are related to the density via the Gladstone-Dale equation. The refractive index is integrated over the line of sight, and the background movement is a function of the first derivative of the density, with the x- and y-components separable in the image plane. The second derivative of the density can be acquired by differentiating the background movement during post-processing, see Settles (2018). This is often used for BOS vortex detection to highlight the vortex core and to remove a constant overall image shift, e.g. due to camera vibration, see Bauknecht et al. (2016).

In contrast to classical schlieren techniques, the BOS technique has several drawbacks, as detailed by Settles and Hargather (2017):

1. The evaluation window size limits the minimum size of object which can be visualized by a given setup, imposing a spatial filter on the data.
2. The requirement for a reference image with undisturbed flow can be difficult to realize for some test cases.
3. The requirement to focus on the background leads to an irreducible blur of the imaged object, imposing an additional spatial filter on the data.
4. Additionally, to the comments by Settles and Hargather, the requirement to size and print a separate background for each experiment (excepting where natural backgrounds are used (Bauknecht et al., 2014) can be onerous.

For point 1, the size of the essential evaluation window is a function of the signal to noise level of the images, but also generally several background dots will be required to get a good cross-correlation peak. One approach to overcome this requirement for steady flows is to use optical flow algorithms for the analysis of a series of BOS images, as detailed by Hill and Haering (2017) for an aircraft flying in front of the sun, and by Smith et al. (2017) for BOS from a follower aircraft. As noted in those papers, a problem with optical flow algorithms as currently implemented is a reduced robustness compared with window cross-correlation.

For point 2, the reference-free digital shadowgraphy method using a moving BOS background with small time difference can be used (Gardner et al., 2020), as demonstrated additionally in this paper. An alternative would be the reference-free BOS method (Bauknecht et al., 2016) where larger time differences cause the schlieren objects in the second image to move onto undisturbed background in the first image and vice-versa, creating a double-image.

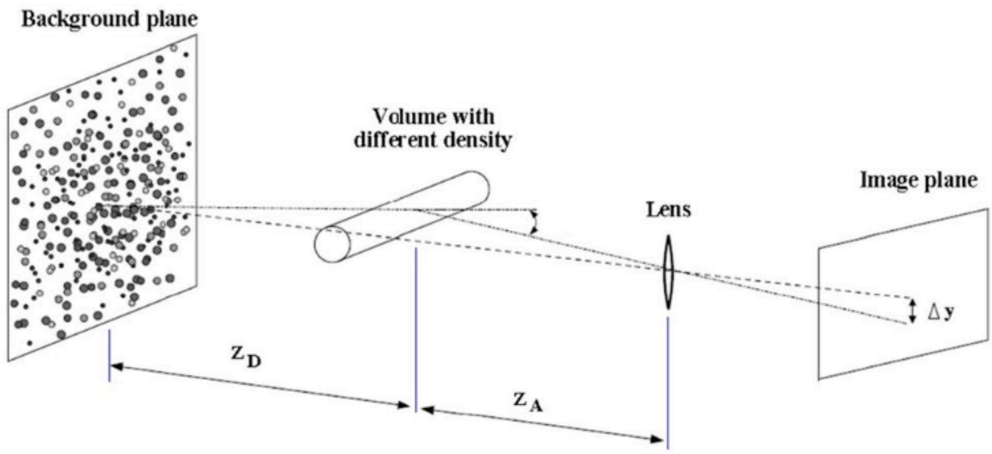


**Fig. 1** Recording principal of the conventional background oriented schlieren method BOS (Raffel 2000)

For point 4, this paper suggests the use of projected backgrounds, which can be dynamically sized, both in field size (slide projection), or in field size and coarseness (speckle projection). This avoids the necessity of printing backgrounds, and allows the dynamic movement of the background if desired.

For point 3, a suggestion for *forward BOS* using projected backgrounds is shown in this paper. If the projected speckle pattern shines through the density object, then the point movement takes place before the speckle strikes the screen. A camera focused on the screen can then record the movement of the speckle, without being subject to the irreducible blur incurred by BOS. In contrast to standard shadowgraphy, this technique is robust when the lighting of the field is uneven, and the point movement is related to the first derivative of density.

## 2. Projected moving background pattern BOS

The BOS method proposed here uses a projection of a point image from a photographic slide to prepare the background as required in Fig. 1. Additionally, the background pattern is moved over time using a rotating mirror in the projection system. As seen in Fig. 2, if the position of an individual fraction of the projected background pattern moves between two image recordings because of the rotating mirror, it will be seen through a different part the density object. This can either be evaluated as reference-free digital shadowgraphy using a moving BOS background as presented by Gardner et al. (2020) or as BOS or knife edge images by various techniques as described in the following. If a series of images is taken over a time frame in which the flow can be considered steady, either by using fast acquisition, or a steady flow, then the ensemble correlation of Meinhart et al. (2000) can be used to reduce the window size to the range $4 \times 4 - 8 \times 8$ pixels. A similar subtraction method is visible in Settles and Hargather (2017), however the moving background method used here is new. Multiple images have been used previously for schlieren velocimetry by Mittelstaedt et al. (2010), but here the ensemble correlation was not used. The AIRBOS method of Smith et al. (2017) used optical flow algorithms to get similar results, but used no projection to generate the motion of background patterns.

The setup for the moving projected background pattern test on a burning candle consisted of a rotating mirror system, a Phantom VEO 640 camera recording at a framerate of 3 kHz at an image size of 1024 x 1600 pixel. The exposure time was set to 150 µs. The lens was a Nikkor with f=50 mm focal length set to an aperture leading to a f-number of 8. The distance camera-to-candle was 0.80 m, the distance camera-to-background was 1.60 m. Background pattern was generated by a slide projector and a slide of a random dot background pattern. The rotating mirror was operated at 0.33 revs/sec. The background pattern moved approximately 8.5 px in the image plane between two subsequent recordings. A series of 201 images has been recorded for the evaluation, yielding a total of 200 results containing the background displacement between subsequent images.

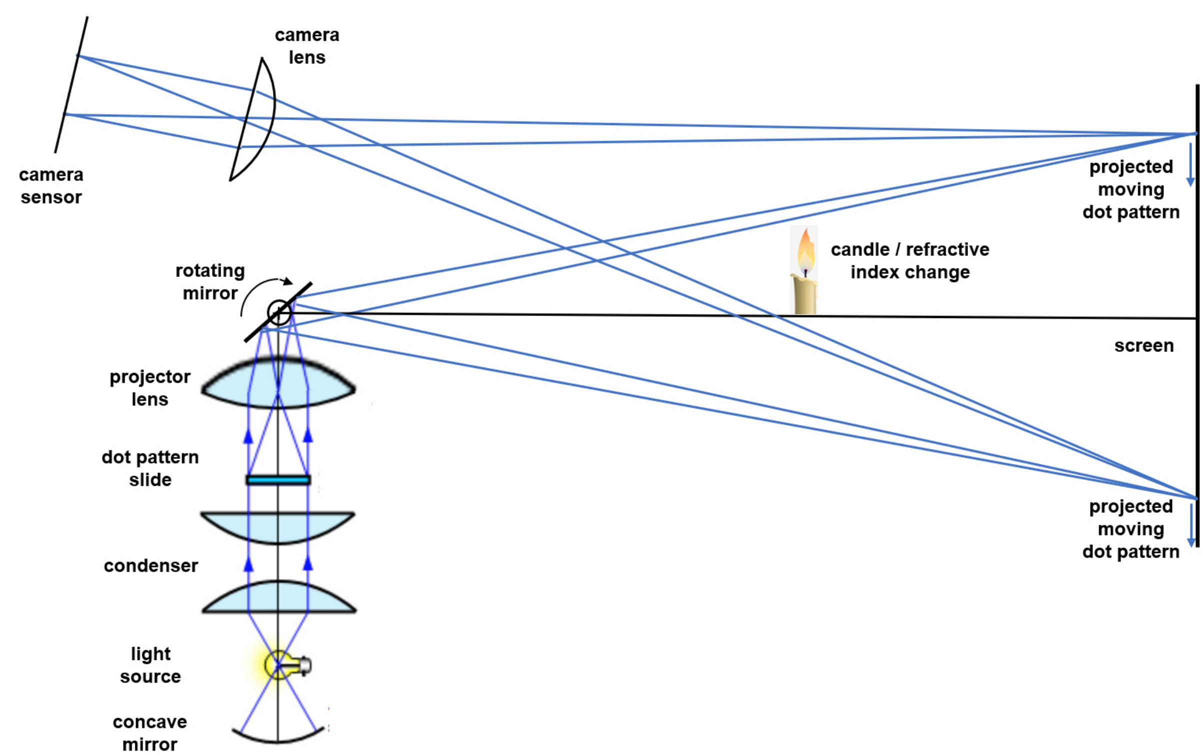


**Fig. 3** Moving background pattern setup for reference-free BOS

Optical flow is the apparent motion between images due to changes in brightness. We use a regularization-based Horn-Schunck (1981) type algorithm to determine the displacement between image pairs. A penalty function of the velocity gradients is weighted against a brightness constancy term which is used to enforce smoothness. Due to the large background displacement between images, a coarse-to-fine pyramidal scheme is required. Image pyramids (Adelson et al. 1984) are constructed for each image pair. The solution is calculated on the coarsest level, and the optical flow at each level is used to warp the second image towards the first image on the next finest scale. A penalty weight of 200 and five pyramid levels are used to compute the flow between image pairs. It has been found that a relatively low penalty weight, while it may lead to increased noise in the individual solutions, can keep from blurring finer scale structures. Increasing penalty weight can have a similar effect as window size in cross-correlation methods; although our experience has shown that weighting is much more subjective and can differ between BOS data sets. This subjectivity of penalty weighting is common to regularization-based methods. It has been observed during the current and previous work that, with the use of multiple backgrounds or solution averaging, this noise can cancel quickly while revealing smaller scale schlieren in cases where they are present.

The results of the more conventional displacement evaluation performed at DLR is based on a sequential cross-correlation performed with the LaVision DaVis 10 software, multi-pass correlation down to 12x12 pixel with 75% overlap. This approach yields a grid spacing of 3 pixel in both x- and y-directions, compared to the single-pixel resolution of the optical flow method.

Figure 4 shows sample results for the horizontal motion, $\Delta x$, and five different evaluation strategies a) to e) using cross-correlation (CC, top row) or optical flow (OF, bottom row). In each result, the candle flame and its plume are in the center. The average right-to-left background motion of about -8.5 pixel was subtracted. The result is in the range between -1.5 and 1.5 pixel, representing the second derivative of the density, $\Delta^2\rho/\Delta x^2$, as argued by (Gardner et al., 2020). Results a) and d) correspond to "simple" instantaneous results derived from two successive camera images N and N+1. Background noise is visible in both results, with slightly less noise in case of the OF evaluation, despite its finer grid resolution (1 pixel versus 3 pixel).

The candle plume is laminar at the bottom and turbulent at the top, but the unsteadiness is slow compared to the image acquisition rate. Hence, the noise can be suppressed at the cost of temporal resolution by combining more than two images via sliding-window methods. Figure 4b) uses a sum-of-correlation ("ensemble correlation", Santiago et al., 1998) approach, averaging the correlation planes in windows sized ±2 results before peak detection. The noise suppression is obvious, while maintaining instantaneous turbulent structures. Averaging instantaneous OF results in a sliding window of the same size yields a comparable result, see Fig. 4e). Figure 4c) repeats the sum-of-correlation approach, additionally accounting for correlations between images N and N+2. This approach can be termed "pyramid level 2" after Sciacchitano et al. (2012). Correlation noise is further suppressed by adding additional correlation planes, but the inherent averaging over longer time spans starts to wash out small-scale turbulent structures.

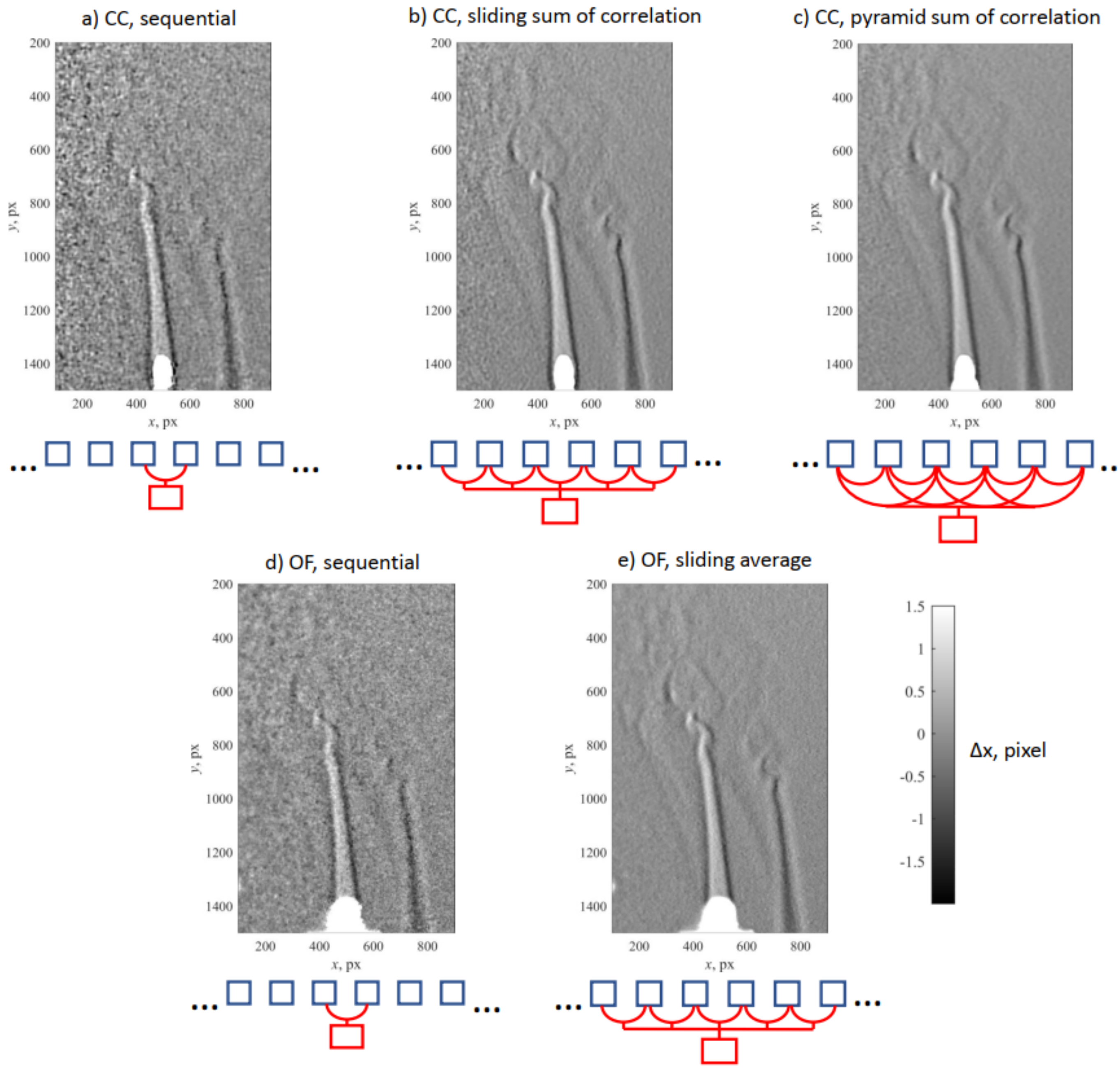


**Fig. 4** Instantaneous results of the candle test case, different evaluation strategies using cross-correlation (CC), top row, and optical flow (OF), bottom row.

It is noted that all results in Fig. 4 contain a shadow-like, mirror-inverted image of the schliere in the right half. This effect will be explained and utilized as "forward BOS" in the next chapter, in which the slide projector is replaced with a pointwise laser light source.

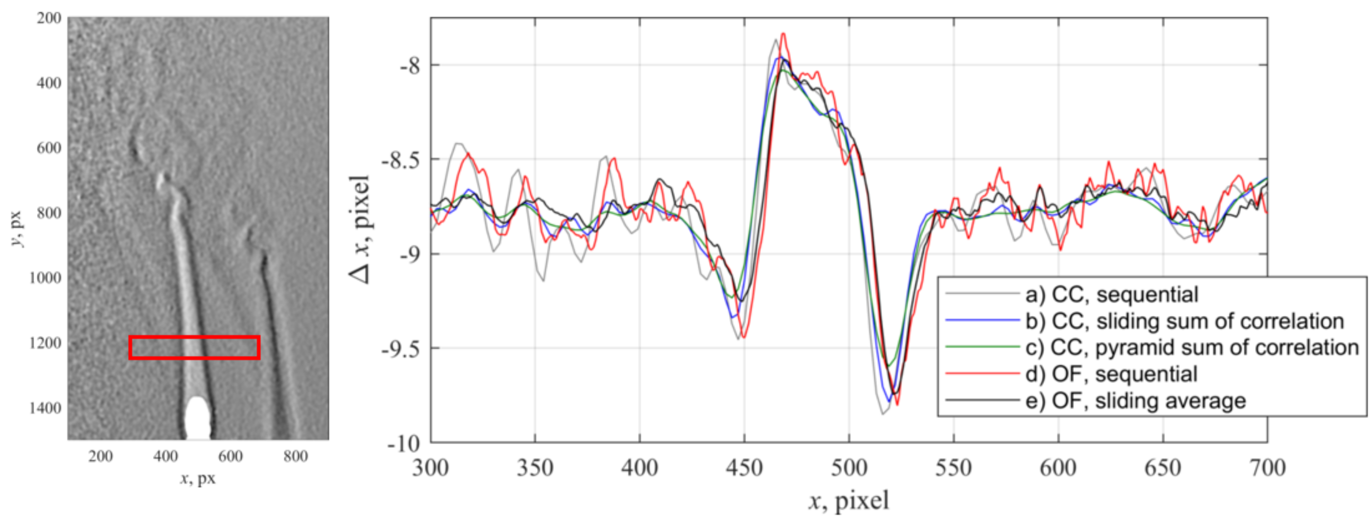


**Fig. 5** Horizontal background motion Δx along coordinate x, extracted and averaged from Fig. 4 between y=1200...1250 pixel.

Figure 5 shows the horizontal background motion versus the horizontal coordinate, extracted and averaged in a laminar region of the flame plume, y=1200…1250 pixel. The labels a) to e) repeat the different evaluation strategies from Fig. 4. The quantitative agreement of all methods is good and supports the earlier observations: The noise level in the instantaneous results, a) and d), can be suppressed by the sliding window techniques, b) and e), but further temporal averaging leads to smaller peak levels, c).

## 3. Laser speckle pattern BOS

The phase object was a horizontal helium jet released from a small plastic tube. The distance camera-to-jet was about 800 mm and the distance between the jet and the background about 400 mm. A sketch of the setup is shown in Fig. 6. The camera field of view included both the image of the tube itself in the lower part (for "standard" BOS schlieren images, jet diffracts rays from background to camera), as well as the shadow of the tube in the upper part. The latter effect, in which the jet diffracts rays from light source to background, will be called "forward" BOS schlieren images in the remainder of this article where. The "forward" BOS images are similar to shadowgraphy, but the laser light transmitted through the phase object contains an intensity pattern generated by a ground glass placed in front of the laser. Adjusting the lenses between the laser and the ground glass allows for the adjustment of the density and size of the projected speckles. The smaller the laser spot on the ground glass the larger are the speckles' sizes and vice versa. Smaller laser spots also lead to a larger depth of field of the projection and therefore allow to vary the location of the density field under investigation to a large extend without noticeable blur neither of the shadow of the nozzle nor of the data. The laser used was a Spectra Physics Excelsior with 250 mW at 532 nm and a beam diameter of 0,32 mm. We used focal lenses of -25 mm and 100 mm and a beam expander. The overall size of the illuminated field can be enlarged with lenses of smaller focal lengths of the lenses.

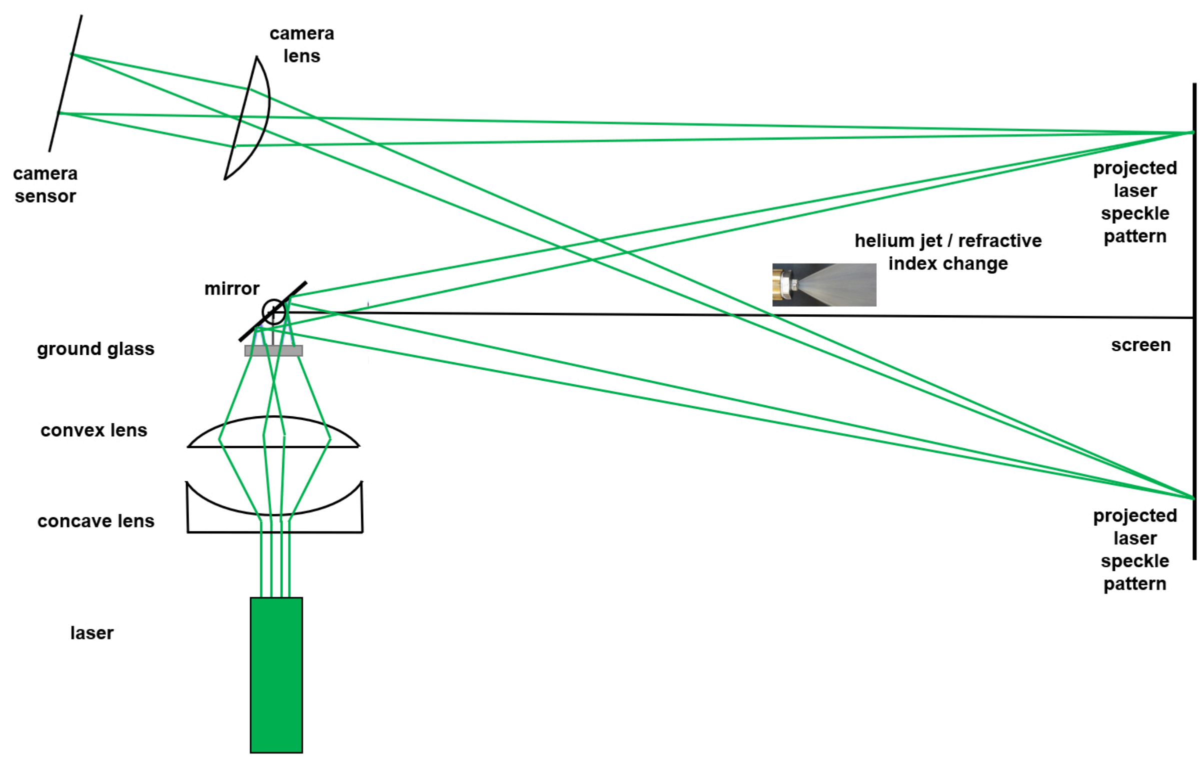


**Fig. 6** Details of the tube's shadow, reference image (top) and measurement image (bottom), f/8.0

Figure 7 compares the relevant parts of the light path for both "standard" (top) and "forward" BOS methods (bottom). Note that the apparent movement of the background pattern as observed by a camera has opposite signs, for example, a low-density phase object attracts background structures in "standard" mode but repels background structures in "forward" mode. This explains the mirror-inverted, shadow-like candle plume already noted in Fig. 4.

The camera used was a Phantom VEO640 (same as for the first candle experiment) at 2 kHz, the lens was a Zeiss Milvus f=100 mm, and the focus was on the background. A rotating mirror was placed in the laser's light path to enable background motion, but in a first step, the mirror was fixed. Hence, the evaluation displays the displacements between the reference image (=helium jet off) and the measurement images (=helium jet on), and the result represents the first derivative of the density (here: $\Delta\rho/\Delta y$) rather than the second derivative ($\Delta^2\rho/\Delta y^2$).

Figure 8 shows two sample images for two different aperture settings of the camera lens, f/8.0 (left) and f/2.8 (right). In both cases, the laser speckle pattern was generated by a ground glass via the non-rotating mirror. The camera was focused on the background and is not collinear with the laser beam but placed above, hence, the image of the jet tube ("standard BOS") and its shadow ("forward BOS") appear above one another. It can be noted that the helium tube for f/2.8 is almost invisible due to the small depth of focus, and that the image of the recording at f/2.8 is much brighter than at f/8.0, despite a reduced exposure time of only 500 $\mu$s compared to 1500 $\mu$s. Both images are shown using the same color coding in a range range of 0….1000 counts.

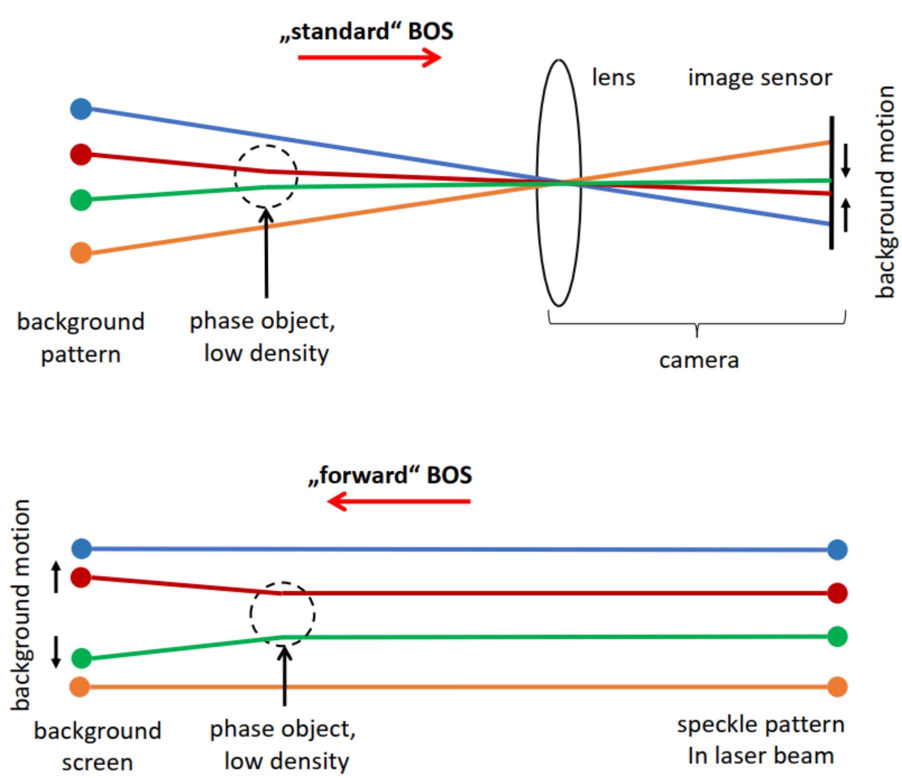


**Fig. 7** Comparison of the principles for "standard" BOS (top) and "forward" BOS (bottom)

Figure 9 depicts three different evaluation results based on a comparison between an instantaneous measurement image versus the jet-free reference image for a non-moving laser speckle background pattern and the aperture setting f/8.0. The coloring corresponds to the vertical background displacement Δy in the range of -1.5...1.5 pixel. The displacement magnitudes of standard BOS (bottom) and forward BOS (top) are similar, since both depend on the distance between the phase object and the background, but the direction is mirror-inverted as predicted in Fig. 7. As a side note, the geometric scaling of the "forward" and "standard" BOS images was not calibrated. In "forward" mode, the image size in the background plane can be modified by the divergence angle of the laser speckle projection, providing an additional degree of freedom complementing the optical magnification of the camera system. However, this effect was not further investigated in the current work.

The cross-correlation in Fig. 9a) used the same parameters as in the candle test case, meaning that the grid resolution is three times lower in both x- and y-directions compared to the optical flow result, Fig. 9b). Nevertheless, both evaluations visualize instantaneous turbulent structures within the jet to a certain degree. A closer look shows that the "forward BOS" result is sharper than the "standard BOS" results, since the camera is focused on the background. The result in Fig. 9c) uses the optical flow algorithm without the pyramidal evaluation scheme as described in Sec. 2.

The results depicted in Fig. 10 represent “simple” (non-ensemble) averages calculated from 500 individual results. The average y-displacement along the y-coordinate is shown in Fig. 11 for two selected areas (red boxes) in the "standard" and "forward" BOS regions. The similar magnitudes but opposite signs for both modes is confirmed, and also the very good quantitative agreement between cross-correlation (red lines) and optical flow with pyramidal scheme (black lines). Omitting the pyramidal scheme (blue lines) leads to an underestimation of the background shift.

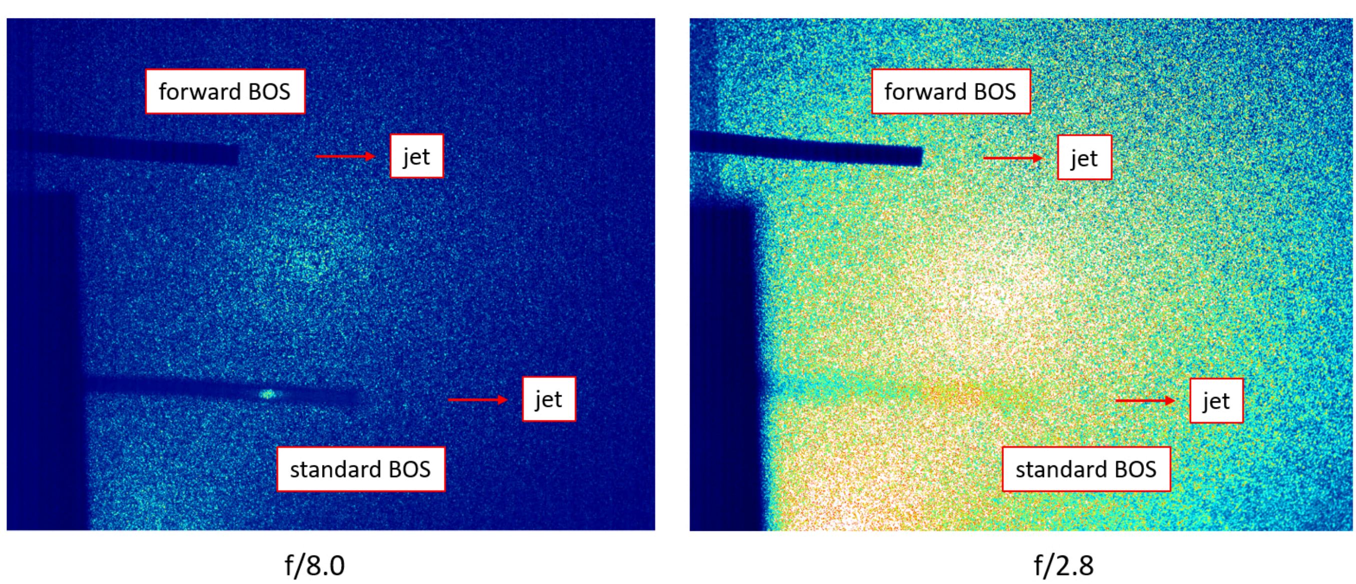


**Fig. 8** Sample camera images of the helium jet and laser speckle background for camera lens apertures f/8.0 (left) and f/2.8 (right). The jet tube and its shadow are visible in separate areas of the image, enabling “standard” and “forward” BOS in the same image

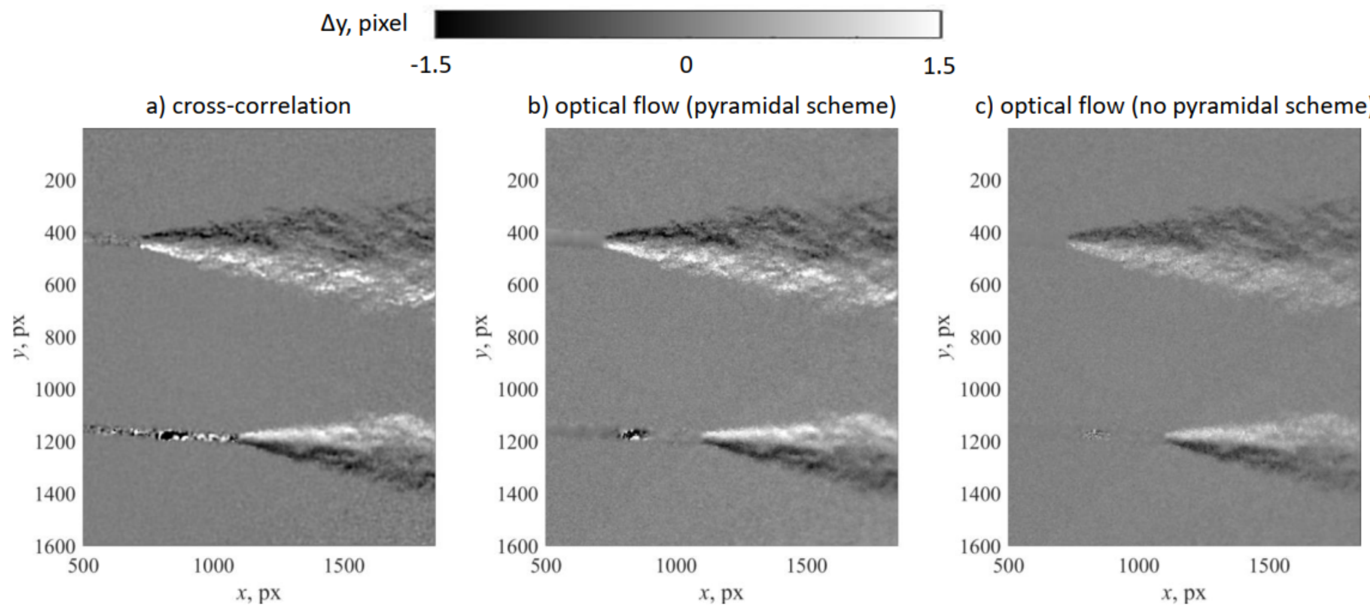


**Fig. 9** Instantaneous sample result of the helium jet, f/8.0

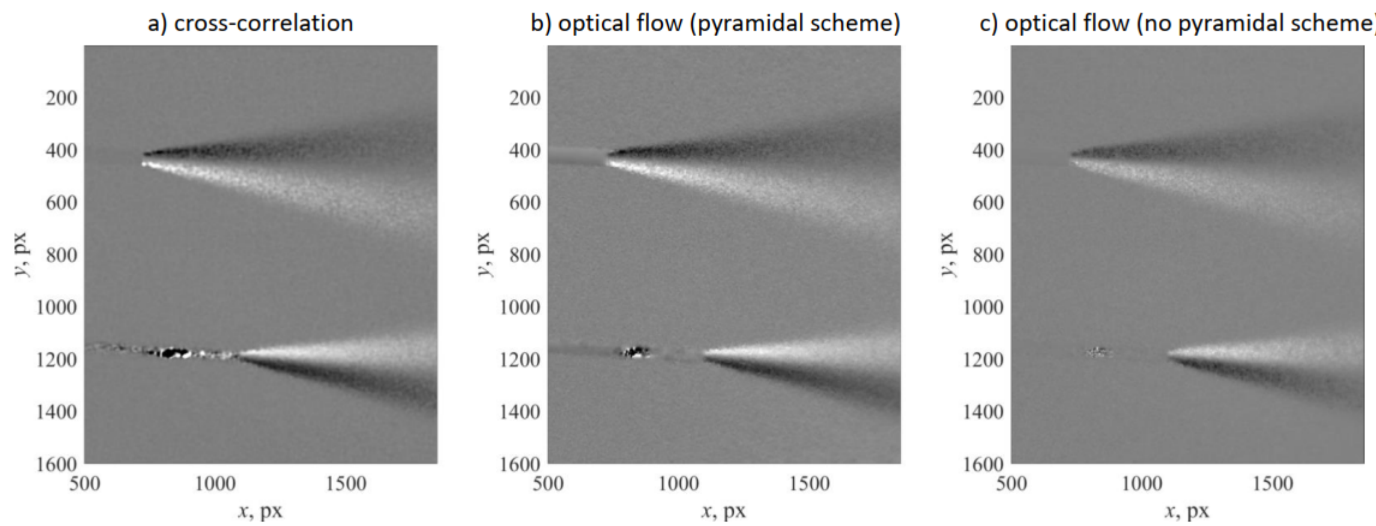


**Fig. 10** Averaged result of the helium jet, 500 individual samples, f/8.0

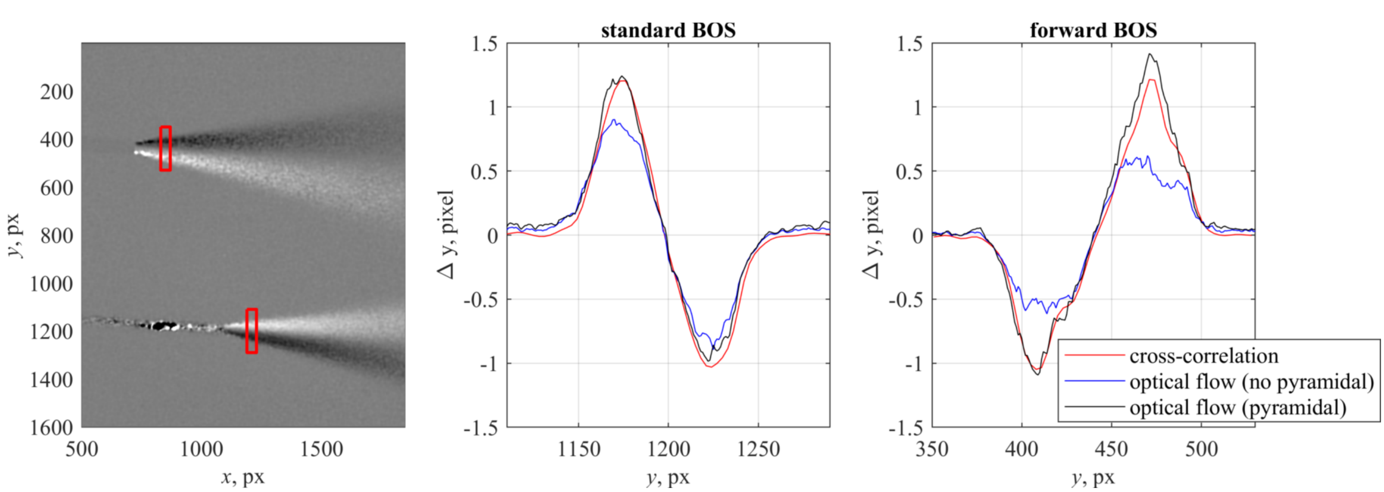


**Fig. 11** Averaged result of the helium jet, 500 individual samples, f/8.0

When opening the aperture from f/8.0 to f/2.8, see Fig. 12, it can be observed that the standard BOS images of the density gradients in the lower half appear blurred and have less signal due to a smaller depth of focus, with the focus set on the background. In contrast, the "forward BOS" mode represented by the displacements in the upper half of the images generates more image displacement (more signal) and, therefore, appear therefore slightly crispier. The reasons are not yet clear, but probably connected to the smaller image exposure times (better representation of instantaneous turbulent structures) and brighter background (better signal-to-noise ratio). The line plots depicted in Fig. 13 compare f/8.0 (dashed lines) and f/2.8 (solid lines), confirming that opening the aperture strongly decreases the standard BOS signal but slightly increases the forward BOS signal. Again, a good quantitative agreement between cross-correlation and optical flow with pyramidal scheme is underlined.

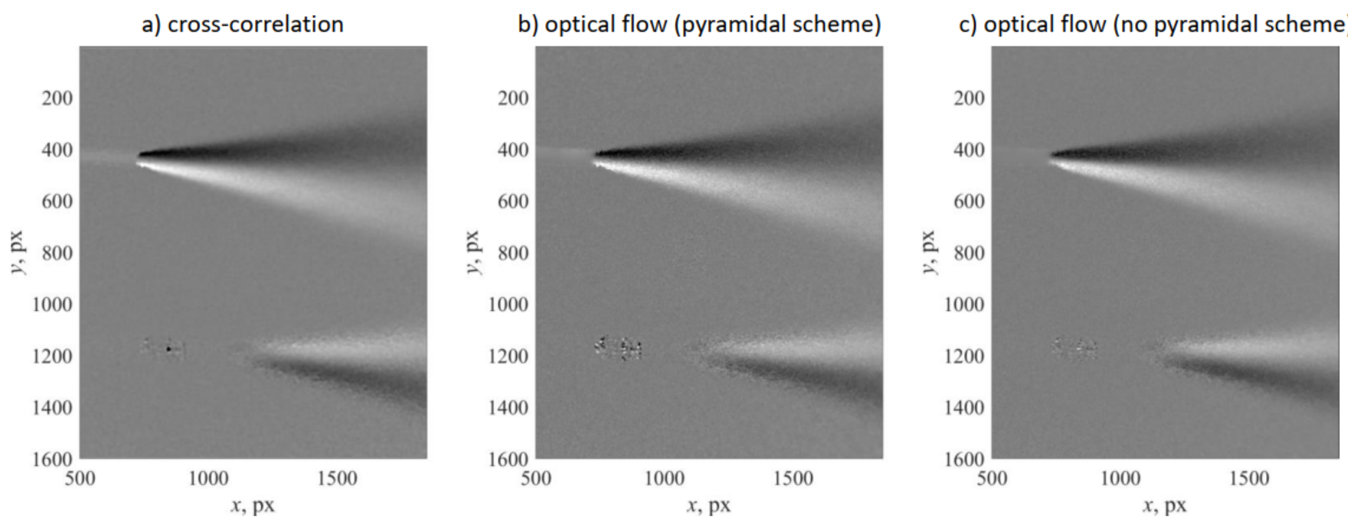


**Fig. 12** Averaged result of the helium jet, 500 individual samples, f/2.8

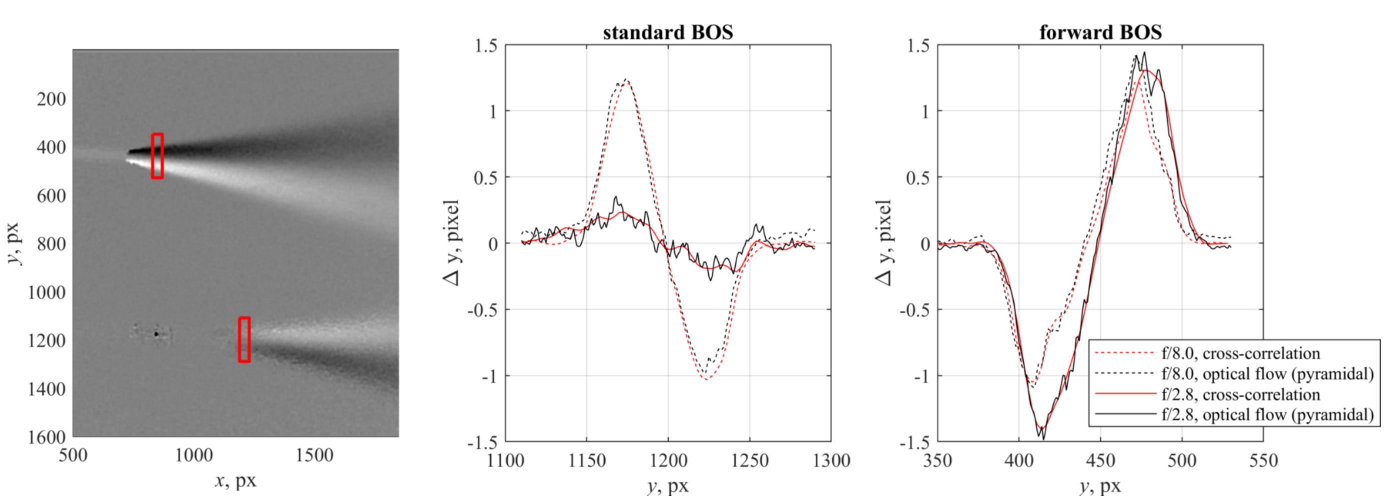


**Fig. 13** Helium jet, comparison of f/2.8 and f/8.0, average result (500 images), vertical line plots

## 5. Conclusions

This paper shows the utility of projected backgrounds for BOS. The main results are:

1. The projected backgrounds can be easily sized according to the measurement requirements, providing a greater flexibility compared to static (e.g. printed) backgrounds.
2. Laser speckle backgrounds provide additional possibilities in terms of illumination intensity or an adjustable background coarseness.
3. The background can be dynamically moved, for example via a rotating mirror, allowing evaluation using the reference-free shadowgraphy or reference-free BOS methods.
4. *Forward BOS* using projected backgrounds is shown in this paper. The projected speckle pattern shines through the density object, and is recorded by a camera focused on the screen. In contrast to standard shadowgraphy, this technique is robust when the lighting of the field is uneven, and the point movement is related to the first derivative of density.
5. Evaluation of the backgrounds with a density object is shown using cross correlation or optical flow analysis of image pairs, showing equivalent results. Ensemble or simple averaging was shown to improve the signal for static flows.

**Acknowledgements**

The authors would like to acknowledge the continuous support of decades of US-German cooperation from NASA and DLR managers.

**6. References**

Adelson, E. H., Anderson, C. H., Bergen, J. R., Burt, P. J., & Ogden, J. M. (1984). Pyramid methods in image processing. RCA engineer, 29(6), 33-41.

Bauknecht A., Merz C.B., Raffel M. (2016) Airborne visualization of helicopter blade tip vortices. J Vis. https://doi.org/10.1007/s1265 0-016-0389-z

Bauknecht A., Merz C.B., Landolt A., Meier A.H., Raffel M. (2014) Blade- tip vortex detection in maneuvering flight using the background- oriented Schlieren technique. J Aircraft. https://doi.org/10.2514/1. C032672

Gardner A.D., Raffel M., Schwarz C., Braukmann J.N., Wolf C.C. (2020) Reference-free digital shadowgraphy using a moving BOS background. Exp. in Fluids https://doi.org/10.1007/s00348-019-2865-4

Hill M.A., Haering E.A. (2017) Ground-to-air flow visualization using solar calcium-K line background-oriented schlieren. Exp Fluids. https://doi.org/10.1007/s00348-016-2285-7

Horn B.K.P. and Schunck B.G. (1981) Determining optical flow. Artificial Intelligence, vol 17, pp 185–203 https://doi.org/10.1115/1.483256

LaVision GmbH (2019) Product manual for DaVis 10.1: flow master D10.1. LaVision GmbH, Göttingen

Meier A.H., Roesgen T. (2013) Improved background oriented schlieren imaging using speckle illumination. Exp. Fluids https://doi.org/10.1007/s00348-013-1549-8

Meinhart C.D., Wereley S.T., Santiago J.G. (2000) A PIV algorithm for estimating time-averaged velocity fields. J Fluids Eng. https://doi. org/10.1115/1.483256

Mittelstaedt E., Davaille A., van Keken P.E., Gracias N., Escartin J. (2010) A noninvasive method for measuring the velocity of diffuse hydro- thermal flow by tracking moving refractive index anomalies. Geochem Geophys Geosyst. https://doi.org/10.1029/2010GC003227

Raffel M. (2015) Background-oriented schlieren (BOS) techniques. Exp Fluids. https://doi.org/10.1007/s00348-015-1927-5

Raffel M., Tung C., Richard H., Yu Y., Meier G.E.A. (2000). Background oriented stereoscopic schlieren (BOSS) for full scale helicopter vortex characterization. 9th International Symposium on Flow Visualization, Edinburgh, UK.

Santiago, J.G., Wereley, S.T., Meinhart, C.D., Beebe, D.J., Adrian, R.J. (1998). A particle image velocimetry system for microfluidics. Exp. Fluids 25. https://doi.org/10.1007/s003480050235

Sciacchitano, A., Scarano, F., Wieneke, B. (2012). Multi-frame pyramid correlation for time-resolved PIV. Exp. Fluids 53. 10.1007/s00348-012-1345-x

Settles G.S. (2018) Smartphone schlieren and shadowgraph imaging. Opt Laser Eng. https://doi.org/10.1016/j.optlaseng.2017.07.002

Settles G.S., Hargather M.J. (2017) A review of recent developments in schlieren and shadowgraph techniques. Meas Sci Technol. https://doi.org/10.1088/1361-6501/aa5748

Smith N.T., Heineck J.T., Schairer E.T. (2017) Optical flow for flight and wind tunnel background oriented schlieren imaging. In: 55th AIAA aerospace sciences meeting, Grapevine, Texas. https://doi. org/10.2514/6.2017-0472